J Radioanal Nucl Chem (2011) 288:467–473
DOI 10.1007/s10967-010-0942-5

Synthesis and biological evaluation of a novel ^{99m}Tc complex of HYNIC-conjugated aminomethylenediphosphonate as a potential bone imaging agent

Liqin Liu · Guangrong Zhong · Yaqian Wei · Min Zhang · Xuebin Wang

Received: 20 November 2010 / Published online: 4 January 2011

Abstract A conjugate of 6-hydrazinopyridine-3-carboxylic acid (HYNIC) with aminomethylenediphosphonic acid (AMDP) was synthesized through a multiple-step reaction. HYNIC–AMDP could be labeled easily and efficiently with ^{99m}Tc using *N*-(2-hydroxy-1,1-bis(hydroxymethyl)ethyl)glycine (tricine) as coligand to form the ^{99m}Tc–HYNIC–AMDP complex in high yield (> 95%). Its partition coefficient indicated that it was a good hydrophilic complex. The biodistribution studies of ^{99m}Tc–HYNIC–AMDP in normal ICR mice showed that this complex had high bone uptake and low or negligible accumulation in non-target organs. As compared with ^{99m}Tc–MDP, ^{99m}Tc–HYNIC–AMDP had a higher bone uptake and the ratios of bone/blood and bone/muscle at early time after injection, suggesting that it could be potentially useful for bone imaging at an earlier time after injection according to further investigations of the biological behavior of this complex.

Keywords Bone imaging agent · Bisphosphonate · ^{99m}Tc · HYNIC · Bifunctional chelator

L. Liu (✉) · G. Zhong · Y. Wei · M. Zhang
Department of Biological Science and Engineering, School of Chemical and Biological Engineering, University of Science and Technology Beijing, 30th Xueyuan Road, Haidian District, Beijing 100083, People's Republic of China
e-mail: liuliqin@ustb.edu.cn

X. Wang
Key Laboratory of Radiopharmaceuticals, Ministry of Education, College of Chemistry, Beijing Normal University, Beijing 100875, People's Republic of China

Introduction

Radionuclide bone imaging is the most common clinical investigation in nuclear medicine. At present the complexes of ^{99m}Tc–MDP [1] and ^{99m}Tc–HMDP [2] are the most widely used tracer agents for clinical radioisotopic bone scanning, whereas they have a number of suboptimal properties. A considerable time interval is required after injection of the radiopharmaceutical before bone scanning can be started. This necessary delay between injection and imaging is a serious inconvenience for the nuclear medicine personnel and for the patients, especially for children. To enable imaging at an earlier time after injection, a radiopharmaceutical with higher affinity for bone is required.

Bisphosphonate analogs accumulate in bone because their phosphonate groups bind to the Ca^{2+} of hydroxyapatite crystals [3]. So the diphosphonate group is necessary both for the complexation of ^{99m}Tc and the uptake of the complex in the skeleton [1]. In the case of ^{99m}Tc–MDP and ^{99m}Tc–HMDP, the phosphonate groups coordinate with technetium [4], which might reduce the ability of binding to the bone surface.

In order to solve this problem, many efforts have been done recently [5–10]. These studies mainly focus on the development of a "new generation" bone imaging agents based on the concept of bifunctional radiopharmaceuticals. The bisphosphonate part of these complexes can be freed and its affinity to the bone can been improved. In this study, 6-hydrazinopyridine-3-carboxylic acid (HYNIC) was chosen as chelating sites because they have been widely used for ^{99m}Tc labeling of proteins, peptides [11–15] and some small molecular compounds [16, 17] on the basis of different coligands and conjugated to aminomethylenediphosphonic acid (AMDP). ^{99m}Tc–HYNIC–AMDP was prepared by coordination with ^{99m}Tc, and their

properties in vitro and in vivo were studied and evaluated as a potential bone imaging agent. In this complex, HYNIC (6-hydrazinopyridine-3-carboxylic acid) was using as a bifunctional chelating agent, so the bisphosphonate part of the complex can be freed and its affinity to the bone can be improved. To the best of our knowledge, this is the first report using the HYNIC–AMDP in the preparation of ^{99m}TcO complex as bone imaging agent.

Experimental

Materials

1,3-Dicyclohexylcarbodiimide (DCC), 1-hydroxybenzotriazole (HOBt) and trimethylsilyl bromide (TMSBr) were obtained from Aldrich Chemical Co. Other chemicals were purchased from Acros Chemical Co. ^{99m}Tc–MDP was prepared by reconstitution with a conventional MDP labeling kit (Beijing Shihong Pharmaceutical Center) with a $^{99m}TcO_4^-$ solution. ^{1}H-NMR spectra were collected on a Bruker 500 MHz FT-NMR spectrometer. ESI–MS were performed on API-3000 LC/MS. $Na^{99m}TcO_4$ was obtained from a commercial ^{99}Mo/^{99m}Tc generator, Beijing Atomic High-tech Co. ICR mice (weighing 20–25 g) was obtained from the Animal Center of Peking University.

Synthesis of HYNIC–AMDP

6-(*Tert*-butoxycarbonyl)-hydrazinopyridine-3-carboxylic acid (Boc-HYNIC) and tetraethyl ester of aminomethylenediphosphonic acid (AMDPE) were synthesized according to procedures described elsewhere [18, 19].

Tetraethyl ester of aminomethylenediphosphonic acid (AMDPE, 0.61 mg, 2.0 mmol) was dissolved in 10 mL dry DMF, then 6-(*tert*-butoxycarbonyl)-hydrazinopyridine-3-carboxylic acid (Boc-HYNIC) (0.66 g, 2.6 mmol) and 1-hydroxybenzotriazole (HOBt) (0.35 g, 2.6 mmol) were added. The solution was cooled to 0 °C and 1,3-dicyclohexylcarbodiimide (DCC) (0.54 g, 2.6 mmol) was added. The reaction mixture was stirred for 30 min at 0 °C and then over night at room temperature. White precipitate was removed by filtration. Next, the solvent was evaporated under reduced pressure giving the crude product. After purification by column chromatography using a dichloromethane : methanol (30:1, v/v) solvent system, the solvent was removed under reduced pressure to provide pure 1-[6-(*tert*-butoxycarbonyl)-hydrazinopyridine-3-carbonyl]-amino-1,1-diphosphonate tetraethyl ester (Boc-HYNIC–AMDPE, 0.48 g, 45%). ^{1}H-NMR ($CDCl_3$): δ 8.64 (s, 1H), 8.06 (s, 1H), 7.89–7.71 (m, 1H), 7.46–7.37 (m, 1H), 6.79 (s, 1H), 5.35 (m, 1H), 4.24–4.20 (m, 8H), 1.47 (s, 9H), 1.38–1.29 (m, 12H); MS (ESI): $[M + H]^+$ 539.4.

To a solution of 1-[6-(*tert*-butoxycarbonyl)-hydrazinopyridine-3-carbonyl]amino-1,1-diphosphonate tetraethyl ester (Boc-HYNIC–AMDPE, 0.22 g, 0.4 mmol) in CH_2Cl_2 (10 mL) at 0 °C was added trimethylsilyl bromide (TMSBr, 1 mL, 7.5 mmol). After stirring at room temperature for 72 h, the reaction mixture was evaporated, and to the residue was added methanol (10 mL). After stirring during 1.5 h, the methanol was removed by evaporation, and the residue was dried in a vacuum over P_2O_5 to obtain crude 1-[6-(*tert*-butoxycarbonyl)-hydrazinopyridine-3-carbonyl]amino-1,1- diphosphonic acid (Boc-HYNIC–AMDP). After addition of a mixture of methanol (5 mL) and 3 M HCl (1 mL), the mixture was stirred during 30 min. The solvent was evaporated, and the residual solid was stirred in methanol (10 mL). The white precipitate was filtered off, washed with methanol, and dried under a stream of nitrogen to yield 1-(6-hydrazinopyridine-3-carbonyl)amino-1,1-diphosphonic acid (HYNIC–AMDP, 0.095 g, 71%) as white crystals. ^{1}H-NMR (D_2O): δ 8.02(s,1H), 7.81 (d, 1H), 6.74 (d, 1H), 5.15 (m, 1H); MS (ESI): $[M + H]^+$ 327.1.

Labeling of HYNIC–AMDP

The radiolabeling of HYNIC–AMDP with ^{99m}Tc using tricine as coligand was performed by adding 0.5 mL solution of tricine (100 mg/mL in 0.9% saline) and 0.5 mL of $SnCl_2$ solution (0.5 mg/mL in 0.1 N HCl) to a clean 10 mL vial containing 100 μL of HYNIC–AMDP solution (10 mg/mL in 0.9% saline), and the pH value was adjusted to 8 with 0.1 N HCl and 0.1 N NaOH. Then 1 mL freshly eluted $^{99m}TcO_4^-$ (15 MBq) from a commercial generator was added to that vial and it was kept at 100 °C for 15 min.

Radiochemical purity analysis

The final complexes were analyzed by TLC and HPLC for the radiochemical purity (RCP). The TLC was performed on a polyamide strip and eluted with saline. The reaction mixture was spotted on the start line, then the strip was developed using saline as a developing system. The strips were removed, dried, cut to 1 cm segments, and assayed for the radioactivity using a well-type γ-scintillation counter.

HPLC analysis was carried out with a reversed-phase column (Kromasil 100-5C, 250 × 4.6 mm ^{2}), Shimadzu SCL-10AVP series. The flow rate was 1 mL/min. The mobile phase was isocratic with 80% solvent A (0.2 M phosphate buffer, pH 6.0) and 20% solvent B (methanol) at 0–5 min, followed by a gradient mobile phase going from 20% solvent B at 5 min to 25% solvent B at 15 min and to 30% solvent B at 25 min.

Stability test

The stability of ^{99m}Tc–HYNIC–AMDP was studied by measuring the RCP of the final complexes by HPLC at different times after preparation.

Determination of the partition coefficient (log *P*) for the complex

The octanol/buffer partition coefficient was measured according to the procedure described by Mukherjee et al. [20–22]. The partition coefficient was determined by mixing the complex with an equal volume of 1-octanol and phosphate buffer (0.025 mol/L, pH 7.4) in a centrifuge tube. The mixture was vortexed at room temperature for 1 min and then centrifuged at 5000 rpm for 5 min. The two layers were separated and from each phase 0.1 mL of the aliquot was removed and counted separately in a well γ-counter. Each measurement was repeated three times. Care was taken to avoid cross contamination between the phases. The partition coefficient P was calculated using the following equation:

$$P = (\text{cpm in octanol} - \text{cpm in background})/(\text{cpm in buffer} - \text{cpm in background})$$

Usually the final partition coefficient value was expressed as log *P*.

Biodistribution studies in mice

Biodistribution studies were carried out in ICR mice weighing 20–25 g. The final ^{99m}Tc complex solution (^{99m}Tc–HYNIC–AMDP, ^{99m}Tc–AMDP or ^{99m}Tc–MDP) was diluted to a concentration of 7.4 MBq/mL with saline. Then 0.1 mL of the diluted tracer solution was injected via a tail vein of mice (four groups each of five mice). The mice were sacrificed at 0.5, 1, 2, 3 h post injection and the organs of interested were weighted and counted in a NaI well-type γ-counter. The results were expressed as the percent uptake of injected dose per gram of tissue (%ID/g). Corrections were made for background radiation and physical decay during experiment. All biodistribution studies were carried out in compliance with the national laws related to the conduct of animal experimentation.

Results and discussion

Synthesis of HYNIC–AMDP

HYNIC–AMDP, the precursor of ^{99m}Tc–HYNIC–AMDP, was synthesized through a multiple-step reaction. The Boc-HYNIC–AMDPE was prepared by the coupling of the carboxyl group of Boc-HYNIC with the amino group of AMDPE. Following that, phosphonate esters were removed by addition of trimethylsilyl bromide (TMSBr) for 72 h to give Boc-HYNIC–AMDP, and HYNIC–AMDP was obtained according to the subsequent deprotection of the Boc group by addition of 3 M HCl/CH_3OH for 30 min.The reaction was schematically shown in Scheme 1. All the intermediates and product HYNIC–AMDP were characterized by ^{1}HNMR and MS. AMDP was obtained according to acid hydrolysis of AMDPE. The AMDP was characterized by ^{1}H NMR and MS. ^{1}H NMR (D_2O) δ:3.40 (t,1H, J = 17.9 Hz, P-C<u>H</u>-P). MS (ESI): $[M]^+$ 227.6.

Labeling of HYNIC–AMDP

^{99m}Tc–HYNIC–AMDP was prepared by a one-pot reaction of HYNIC–AMDP with $^{99m}TcO_4^-$ and tricine in the presence of $SnCl_2$. The radiochemical purity of ^{99m}Tc–HYNIC–AMDP was more than 95%.

^{99m}Tc–MDP was prepared by reconstitution with a conventional MDP labeling kit (Beijing Shihong Pharmaceutical Center) with a $^{99m}TcO_4^-$ solution. AMDP was directly radiolabeled with ^{99m}Tc using $SnCl_2$ as reducing agent at room temperature.

Radiochemical purity analysis

The radiochemical purity of the ^{99m}Tc–HYNIC–AMDP was routinely checked by TLC and HPLC. By TLC, in saline, the free $^{99m}TcO_4^-$ and $^{99m}TcO_2{\cdot}nH_2O$ remained near the origin with R_f = 0.0–0.1, while ^{99m}Tc–HYNIC–AMDP migrated with the solvent front with R_f = 0.8–1.0. An HPLC radiochromatogram was presented in Fig. 1. It was observed that the retention time of $^{99m}TcO_4^-$ was 3.5 min, while that of ^{99m}Tc–HYNIC–AMDP was found to be 12.7 min. Single peak suggested only one product (^{99m}Tc–HYNIC–AMDP) was formed. The mean radiochemical purity of the product was over 95% immediately after the preparation.

The radiochemical purity of ^{99m}Tc–AMDP and ^{99m}Tc–MDP was determined by TLC on polyamide strip eluted with saline. $^{99m}TcO_2{\cdot}nH_2O$ and $^{99m}TcO_4^-$ remained at the origin while ^{99m}Tc–AMDP/^{99m}Tc–MDP migrated with the front. The radiochemical purity of ^{99m}Tc–AMDP and ^{99m}Tc–MDP were both over 95% after preparation.

Stability test

The stability of ^{99m}Tc–HYNIC–AMDP was studied by measuring the RCP at different times after preparation. Its

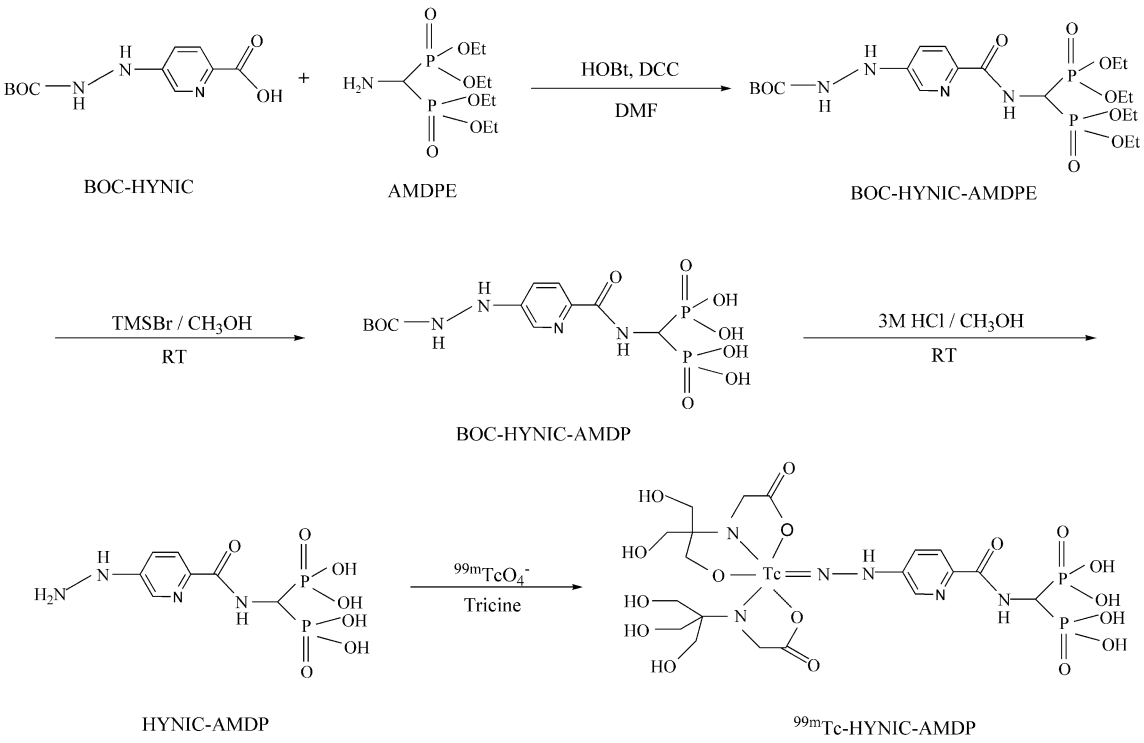

Scheme 1 Synthesis of HYNIC–AMDP and Preparation procedure of ^{99m}Tc–HYNIC–AMDP

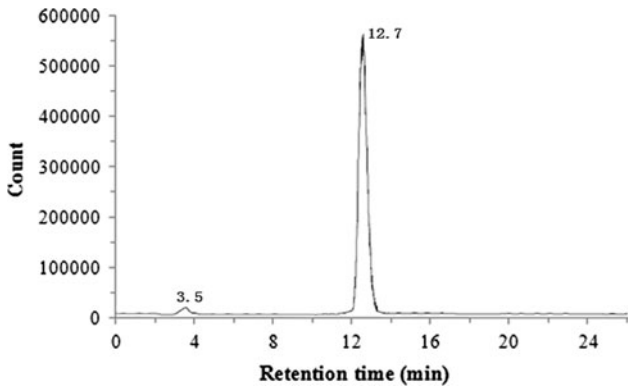

Fig. 1 HPLC radiochromatogram of ^{99m}Tc–HYNIC–AMDP

radiochemistry purity was more than 90% after 6 h, which indicated the complex possesses a great stability in the reaction mixture at room temperature.

Determination of the partition coefficient (log *P*) for the complex

The partition coefficient (log *P*) values of ^{99m}Tc–HYNIC–AMDP and ^{99m}Tc–AMDP at pH 7.4 were −2.77 and −1.52 respectively, suggesting two complexes were highly hydrophilic and ^{99m}Tc–HYNIC–AMDP was more hydrophilic than ^{99m}Tc–AMDP.

Biodistribution studies in mice

The results of biodistribution of ^{99m}Tc–HYNIC–AMDP, ^{99m}Tc–AMDP and ^{99m}Tc–MDP were presented in Tables 1, 2 and 3 separately.

As described in Table 1, ^{99m}Tc–HYNIC–AMDP had a high bone uptake and good target/non-target ratios. The B/B and B/M ratios increased from 1–3 h post injection. The kidney uptake was much higher than the hepatic. Early

Table 1 Biodistribution of ^{99m}Tc–HYNIC–AMDP in ICR mice (%ID/g)

Tissues	0.5 h	1.0 h	2.0 h	3.0 h
Heart	0.48 ± 0.11	0.33 ± 0.06	0.25 ± 0.02	0.37 ± 0.03
Liver	2.19 ± 0.39	2.28 ± 0.44	1.36 ± 0.39	1.30 ± 0.12
Spleen	0.79 ± 0.07	1.07 ± 0.23	0.32 ± 0.07	0.28 ± 0.06
Lung	0.56 ± 0.19	0.41 ± 0.09	0.29 ± 0.04	0.21 ± 0.02
Kidney	3.24 ± 0.56	1.76 ± 0.30	1.12 ± 0.20	0.59 ± 0.15
Muscle	0.55 ± 0.06	0.68 ± 0.05	0.26 ± 0.02	0.16 ± 0.01
Bone	44.18 ± 8.58	35.08 ± 4.92	36.71 ± 4.99	32.41± 4.28
Blood	0.70 ± 0.01	0.38 ± 0.02	0.21 ± 0.03	0.18 ± 0.01
B/M	80.33	51.59	141.19	202.56
B/B	63.11	92.32	174.81	180.06

All data are the mean percentage ($n = 5$) of the injected dose of ^{99m}Tc–HYNIC–AMDP per gram of tissue, ± the standard deviation of the mean

B/M bone-to-muscle, B/B bone-to-blood

Table 2 Biodistribution of ^{99m}Tc–AMDP in ICR mice (%ID/g)

Tissues	0.5 h	1.0 h	2.0 h	3.0 h
Heart	0.96 ± 0.14	0.59 ± 0.09	0.53 ± 0.06	0.23 ± 0.02
Liver	26.93 ± 2.81	31.89 ± 2.82	29.06 ± 1.81	28.53 ± 1.97
Spleen	44.01 ± 4.75	34.63 ± 7.50	44.59 ± 8.00	39.41 ± 8.26
Lung	10.55 ± 2.90	6.08 ± 1.27	1.53 ± 0.33	1.40 ± 0.38
Kidney	8.45 ± 2.48	7.33 ± 2.30	9.13 ± 1.87	8.22 ± 1.99
Muscle	0.28 ± 0.03	0.18 ± 0.02	0.33 ± 0.05	0.08 ± 0.01
Bone	9.05 ± 1.65	7.59 ± 1.60	6.87 ± 0.19	5.54 ± 1.23
Blood	1.59 ± 0.39	0.35 ± 0.08	0.18 ± 0.02	0.13 ± 0.01
B/M	32.58	41.15	21.12	73.80
B/B	5.70	21.88	37.44	42.62

All data are the mean percentage ($n = 5$) of the injected dose of ^{99m}Tc–AMDP per gram of tissue, ± the standard deviation of the mean

B/M bone-to-muscle, B/B bone-to-blood

Table 3 Biodistribution of ^{99m}Tc–MDP in ICR mice (%ID/g)

Tissues	0.5 h	1.0 h	2.0 h	3.0 h
Heart	0.40 ± 0.02	0.27 ± 0.05	0.17 ± 0.02	0.19 ± 0.02
Liver	3.86 ± 0.57	3.82 ± 0.39	1.31 ± 0.09	0.89 ± 0.07
Spleen	3.22 ± 0.45	1.82 ± 0.24	2.13 ± 0.46	3.65 ± 0.67
Lung	1.02 ± 0.21	0.45 ± 0.02	0.53 ± 0.06	0.71 ± 0.08
Kidney	2.48 ± 0.69	1.78 ± 0.25	0.95 ± 0.19	1.08 ± 0.19
Muscle	0.16 ± 0.04	0.12 ± 0.04	0.09 ± 0.01	0.08 ± 0.01
Bone	3.26 ± 0.78	4.79 ± 1.23	3.87 ± 0.55	7.77 ± 0.53
Blood	0.47 ± 0.13	0.28 ± 0.05	0.15 ± 0.02	0.12 ± 0.01
B/M	20.38	39.92	43.00	97.13
B/B	6.94	17.11	25.80	64.75

All data are the mean percentage ($n = 5$) of the injected dose of ^{99m}Tc–MDP per gram of tissue, ± the standard deviation of the mean

B/M bone-to-muscle, B/B bone-to-blood

renal activity reflects urinary elimination of this complex. The uptakes of the tracer in other organs (muscle, lung, heart, and spleen) were within the normal values. As compared with ^{99m}Tc-AMDP, significantly higher bone uptake, B/B and B/M ratios of ^{99m}Tc–HYNIC–AMDP were observed. That indicated that the phosphonate groups maybe do not coordinate with technetium when labeling of HYNIC–AMDP using tricine as coligand, which could be responsible for high bone uptake of ^{99m}Tc–HYNIC–AMDP. Of course, the structure of ^{99m}Tc–HYNIC–AMDP was required to further study. Also, other factors may be influence the bone uptake, so further study could be required to illustrate the mechanism for bone localization.

As compared with ^{99m}Tc–MDP, ^{99m}Tc–HYNIC–AMDP had much higher bone uptake and B/B and B/M ratios. The comparison of biodistribution of ^{99m}Tc–HYNIC–AMDP with ^{99m}Tc–MDP at 1 h post injection was shown in Fig. 2.

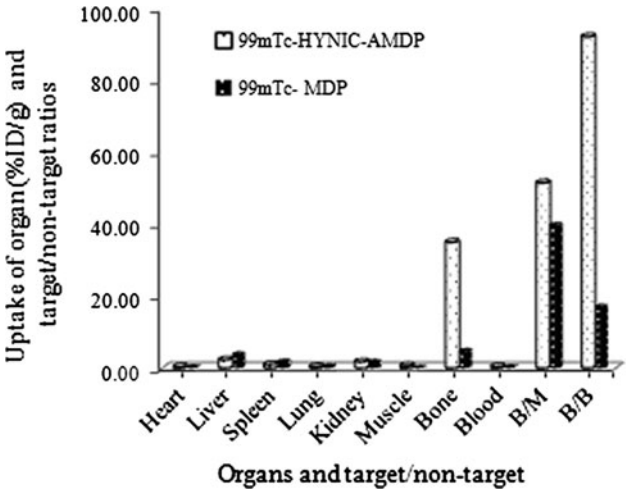

Fig. 2 The comparison of biodistribution of ^{99m}Tc–HYNIC–AMDP and ^{99m}Tc–MDP at 1 h post injection

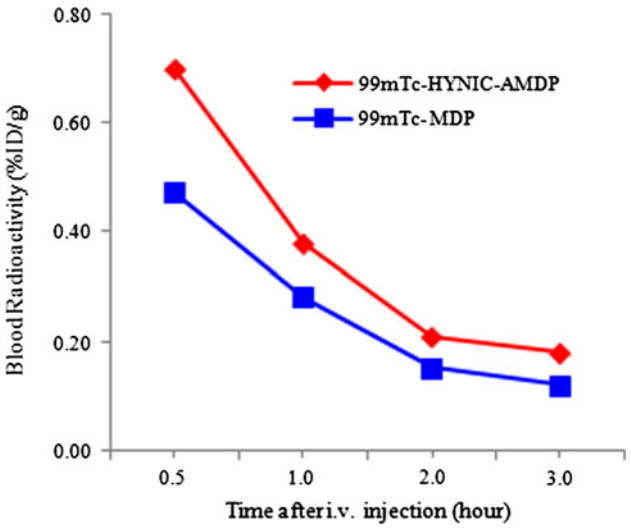

Fig. 3 Blood clearance curves of ^{99m}Tc–HYNIC–AMDP and ^{99m}Tc–MDP

As seen from Fig. 2, the bone uptake and the ratios of B/B and B/M of ^{99m}Tc–HYNIC–AMDP is obviously much higher than the results of ^{99m}Tc–MDP at 1 h post injection, and the uptakes of ^{99m}Tc–HYNIC–AMDP in other organs (muscle, lung, heart, and spleen) were similar to the ^{99m}Tc–MDP. The comparison of blood clearance of ^{99m}Tc-HYNIC-AMDP with ^{99m}Tc-MDP was presented in Fig. 3. As seen from Fig. 3, the blood clearance of ^{99m}Tc–HYNIC–AMDP (from 0.70 ± 0.01 at 0.5 h to 0.38 ± 0.02%ID/g at 1 h post injection) was slightly faster than that of ^{99m}Tc–MDP(from 0.47 ± 0.13 at 0.5 h to 0.28 ± 0.05%ID/g at 1 h post injection) at early time after injection. By comparison, ^{99m}Tc–HYNIC–AMDP is superior to ^{99m}Tc–MDP with regard to the bone uptake and the B/M and B/B ratios at early time after injection, which suggested that it could

Table 4 Comparison of biodistribution of ^{99m}Tc–HYNIC–AMDP with some reported ^{99m}Tc-chelate-conjugated bisphosphonate derivatives

Complex	^{99m}Tc–HYNIC–AMDP	^{99m}Tc–MAG_3–HBP	^{99m}Tc–EC–AMDP	^{99m}Tc–Gem/BP
Animal	ICR mice	Wistar Rats	Rats	BALB/c mice
Weight	20–25 g	200–230 g	60–80 g	20–22 g
Time p.i. (h)	1	1	1	1
Bone uptake (%ID/g)	35.08 ± 4.92	4.23 ± 0.25	14.8	20.81±2.90
B/B ratio	92.32	59.7	55.1	3.48
Reference	Present study	7	5	10

be potentially useful for bone imaging at an earlier time after injection according to further investigations of the biological behavior of this complex.

The comparison of biodistribution of ^{99m}Tc–HYNIC–AMDP with some reported ^{99m}Tc–chelate–conjugated bisphosphonate derivatives was shown in Table 4. Although the animal species used in biodistribution studies of the ^{99m}Tc-complexes listed in Table 4 were slightly different, the amount of bone uptake and the ratio of B/B can be seen roughly. As seen from Table 4, ^{99m}Tc–HYNIC–AMDP exhibited the highest bone uptake (35.08 ± 4.92%ID/g at 1 h p. i.) and B/B ratio (92.32 at 1 h p. i.) at early time after injection among the four complexes. A decrease of B/B ratio in the order was observed: ^{99m}Tc–HYNIC–AMDP > ^{99m}Tc–MAG_3–HBP > ^{99m}Tc–EC–AMDP > ^{99m}Tc–Gem/BP. And the order of the bone uptake was ^{99m}Tc–HYNIC–AMDP > ^{99m}Tc–Gem/BP > ^{99m}Tc–EC–AMDP > ^{99m} Tc–MAG_3–HBP. Compared with ^{99m}Tc–EC–AMDP (using EC as bifunctional chelator), the bone uptake (35.08 ± 4.92%ID/g at 1 h p. i.) and B/B ratio (92.32 at 1 h p. i.) of ^{99m}Tc–HYNIC–AMDP (using HYNIC as bifunctional chelator) were obviously much higher. Also, the biodistribution of ^{99m}Tc–HYNIC–AMDP in normal mice pointed to the possibility of the use of this tracer as bone imaging agent. However, many biological studies are required to establish these findings as the examination of the tracer in the skeletal lesions and normal bone and the quantitative determination of the tissue uptake of this tracer.

Conclusion

In summary, the novel HYNIC-conjugated aminomethylenediphosphonate ligand HYNIC–AMDP has been successfully synthesized and ^{99m}Tc–HYNIC–AMDP was prepared in high yields using tricine as coligand. The high bone uptake, good retention and high target to non-target activity ratios of the ^{99m}Tc–HYNIC–AMDP in normal mice exhibited favorable properties, especially ^{99m}Tc–HYNIC–AMDP had a higher bone uptake and bone/blood ratio at early time after injection than ^{99m}Tc–MDP, suggesting that it could be potentially useful for bone imaging at an earlier time after injection according to further investigations of the biological behavior of this complex.

Acknowledgments The work was financially supported by the Fundamental Research Funds for the Central Universities of China (FRF-BR-09-006A) and by the International Science and Technology Cooperation Program of China(ISTCP) (2008AR), the Ministry of Science and Technology of the People's Republic of China. The radiochemical data were acquired at Key Laboratory of Radiopharmaceuticals (Beijing Normal University), Ministry of Education.

References

1. Subrahamian G, McAfee JG, Blair RJ, Kollfelz FA, Thomas FP (1975) J Nucl Med 16:744–755
2. Domstad PA, Coupal JJ, Kim EE, Blake JS, DeLand FH (1980) Radiology 136:209–211
3. Meyer JL, Nancollas GH (1973) Calcif Tissue Res 13:295–303
4. Libson K, Deutsch E, Barnett BL (1980) J Am Chem Soc 102:2476–2478
5. Verbeke K, Rozenski J, Cleynhens B, Vanbilloen H, De Groot T, Weyns N, Bormans G, Verbruggen A (2002) Bioconjug Chem 13:16–22
6. Liu L, Guo H, Tang Z, Lu J, Wang X (2005) J Label Compd Radiopharm 48:S254
7. Ogawa K, Mukai T, Inoue Y, Ono M, Saji H (2006) J Nucl Med 47:2042–2047
8. Liu W, Hajibeigi A, Lin M, Rostollan CL, Kovacs Z, Orhan K, Sun XK (2008) Bioorg Med Chem Lett 18:4789–4793
9. Panwar P, Singh S, Kumar N, Rawat H, Mishra AK (2007) Bioorg Med Chem 15:1138–1145
10. El-Mabhouh AA, Angelov CA, Cavell R, Mercer JR (2006) Nucl Med Biol 33:715–722
11. Liu S, Edwards DS, Barrett JA (1997) Bioconjug Chem 8:621–636
12. Abrams MJ, Juweid M, TenKate CI, Schwartz DA, Hauser MM, Gaul FE, Fuccello AJ, Rubin RH, Strauss HW, Fischman AJ (1990) J Nucl Med 31:2022–2028
13. Ohtsuki K, Akashi K, Aoka Y, Blankenberg FG, Kopiwoda S, Tait JF, Strauss HW (1999) Eur J Nucl Med 26:1251–1258
14. Steffens MG, Oosterwijk E, Kranenborg MHGC, Manders JMB, Debruyne FMJ, Corstens FHM, Boerman OC (1999) J Nucl Med 40:829–836
15. Lambrecht FY, Durkan K, Bayrak E (2010) J Radioanal Nucl Chem 284:539–545
16. Liu LQ, Zhang M, Zhong GR, Wang XB (2010) J Radioanal Nucl Chem. doi:10.1007/s10967-010-0889-6
17. Guo W, Hinkle GH, Lee RJ (1999) J Nucl Med 40:1563–1569
18. Ono M, Arano Y, Mukai T, Fujioka Y, Ogawa K, Uehara T, Saga T, Konishi J, Saji H (2001) Nucl Med Biol 28:215–224

19. Darko K, Kane DJ, William JW (1996) Synth Commun 26:2037–2043
20. Misra M, Sarkar HS, Chakravarty M, Sanyal S, Ganguly S (1994) Nucl Med Commun 15:878–885
21. Zhang JB, Yu Q, Huo JF, Pang Y, Yang S, He YI, Tang TT, Yang CC, Wang XB (2010) J Radioanal Nucl Chem 283:481–485
22. Mukherjee S, Chatterjee J, Punyabrata D, Sengupta C, Banerjee S (1993) J Nucl Med 20:413–426